

# Palladium-Catalyzed Ring Expansion of Spirocyclopropanes to Form Caprolactams and Azepanes

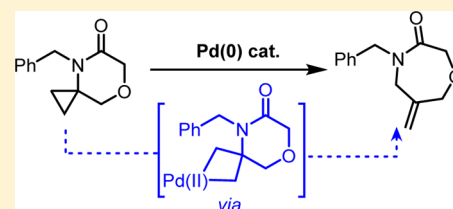
Olivier René,<sup>\*,†</sup> Iain A. Stepek,<sup>†,§</sup> Alberto Gobbi,<sup>†</sup> Benjamin P. Fauber,<sup>†</sup> and Simon Gaines<sup>‡</sup>

<sup>†</sup>Genentech, Incorporated, Discovery Chemistry, 1 DNA Way, South San Francisco, California 94080, United States

<sup>‡</sup>Argenta, Discovery Services, Charles River, 7-9 Spire Green Centre, Flex Meadow, Harlow, Essex CM19 5TR, United Kingdom

**S** Supporting Information

**ABSTRACT:** A palladium(0)-catalyzed rearrangement of piperidones and piperidines bearing a spirocyclopropane ring was developed. The ring expansion reaction led to a variety of functionalized caprolactam and azepane products in good to excellent yields. Experimental and computational mechanistic studies revealed an initial oxidative addition of the distal carbon–carbon bond of a cyclopropane ring to the palladium(0) catalyst and the relief of ring strain as a driving force for product formation.



## INTRODUCTION

Seven-membered nitrogen-containing heterocycles are prominently featured in biologically active natural products<sup>1</sup> and marketed drugs<sup>2</sup> and play a critical role in material science.<sup>3</sup> Despite the prevalence of this structural motif, slow cyclization kinetics have hindered the development of robust methods for the direct construction of these medium-sized heterocycles.<sup>4</sup> At present, these systems are more commonly accessed via a select few ring-expansion processes, such as migratory shift reactions, cleavage of a shared bond in fused [4.1.0] or [3.2.0] bicyclic systems, and electrocyclization reactions.<sup>5</sup> Further exploration of novel ring-expansion pathways leading to seven-membered nitrogen-containing heterocycles is therefore of interest.

Because of their unique structural and electronic properties, cyclopropanes may undergo transition metal-promoted cleavage of the otherwise inert carbon–carbon bond.<sup>6,7</sup> We envisaged that disubstituted cyclopropane **1** (Figure 1A) could undergo C–C bond cleavage in the presence of a transition metal via one of two postulated mechanistic pathways, both leading to common ring-open  $\pi$ -allyl intermediate **3**. Path A would involve an initial oxidative addition of the C–X bond of cyclopropane **1** to transition metal species [M], giving rise to metallated intermediate **2**. Subsequent C–C bond cleavage via  $\beta$ -carbon elimination<sup>8</sup> would afford  $\pi$ -allyl intermediate **3**. Alternatively, in path B, direct oxidative addition of the distal C–C bond of cyclopropane **1** to the metal would lead to metallacycle intermediate **4**. This intermediate could then undergo rearrangement to  $\pi$ -allyl intermediate **3** through  $\beta$ -elimination of X. In cases where X and Y form part of a spirocyclic piperidone or piperidine ring system, the resulting  $\pi$ -allyl intermediate would represent a ring expanded metallacycle poised to undergo reductive elimination to the corresponding caprolactam or azepane, respectively.

Herein, we report the palladium(0)-catalyzed rearrangement of  $\delta$ -lactams and saturated *N*-heterocycles bearing a spirocyclopropane ring, which furnished the corresponding 7-membered heterocycles (Figure 1B). In addition, the ring-expanded products featured a unique  $\delta$ -exomethylene functionality primed for further

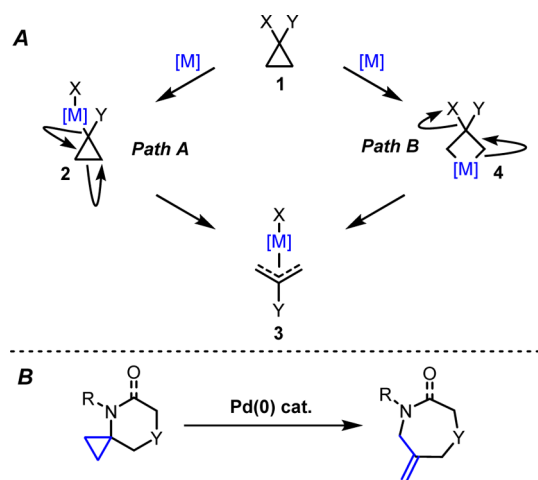


**Figure 1.** Mechanistic pathways for the transition metal-promoted C–C bond cleavage of cyclopropane **1** and Pd(0)-catalyzed rearrangement of lactams and piperidines bearing a spirocyclopropane ring.

late-stage diversification. Experimental and computational mechanistic studies were also performed to elucidate the mechanistic pathway of this transformation. To our knowledge, this is the first reported palladium(0)-catalyzed C–C bond cleavage reaction of a spirocyclic cyclopropane that led to further functionalized ring-expanded products.<sup>9–11</sup>

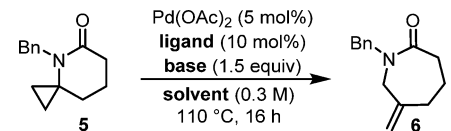
## RESULTS AND DISCUSSION

**Optimization and Scope.** Initial reaction development and optimization on the Pd(0)-catalyzed rearrangement of lactam **5** using Pd(OAc)<sub>2</sub> as a precatalyst revealed the superiority of electron-rich biarylphosphine ligands (Table 1).<sup>12</sup> Although MePhos (Table 1, entry 1) resulted in low conversion to

Received: August 10, 2015

Published: September 17, 2015

Table 1. Optimization of the Reaction Conditions



entry	ligand	base	solvent	conversion <sup>a</sup>
1	MePhos	Cs <sub>2</sub> CO <sub>3</sub>	DMF	12
2	DavePhos	Cs <sub>2</sub> CO <sub>3</sub>	DMF	79
3	RuPhos	Cs <sub>2</sub> CO <sub>3</sub>	DMF	97
4	BINAP	Cs <sub>2</sub> CO <sub>3</sub>	DMF	2
5	PPh <sub>3</sub>	Cs <sub>2</sub> CO <sub>3</sub>	DMF	0
6	RuPhos	no base	DMF	38
7	RuPhos	NaOt-Bu	DMF	0
8	RuPhos	Cs <sub>2</sub> CO <sub>3</sub>	toluene	94
9	<b>RuPhos</b>	<b>Cs<sub>2</sub>CO<sub>3</sub></b>	<b><i>t</i>-AmOH</b>	<b>100</b>
10 <sup>b</sup>	RuPhos	Cs <sub>2</sub> CO <sub>3</sub>	<i>t</i> -AmOH	0

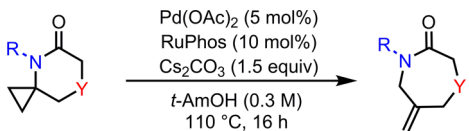
<sup>a</sup>Determined by <sup>1</sup>H NMR analysis of the crude reaction mixture. <sup>b</sup>No Pd(OAc)<sub>2</sub> added.

rearranged caprolactam **6** (12%), as determined by <sup>1</sup>H NMR analysis of the crude reaction mixture, significant improvements were achieved with DavePhos (entry 2) and RuPhos (entry 3), leading to conversions of 79 and 97%, respectively. Conversely, bidentate ligand BINAP (entry 4) and triphenylphosphine (entry 5) resulted in only trace amounts or even no observed formation of product **6**.

Although not necessary for the generation of product **6**, the addition of a base proved critical to achieve complete conversion. For example, although the combination of Pd(OAc)<sub>2</sub> and RuPhos in conjunction with Cs<sub>2</sub>CO<sub>3</sub> gave rise to almost complete conversion (entry 3), the same reaction in the absence of base provided rearranged product **6** in a more modest 38% conversion (entry 6). From these data, it can be inferred that the addition of excess carbonate favored the formation of a stabilized Pd(0)L<sub>n</sub>X<sup>-</sup> anionic complex.<sup>13</sup> This may represent the resting state of the catalyst and would explain the increased observed turnover in the presence of carbonate. Partial decomplexation to a more active Pd(0)L<sub>n-1</sub>X<sup>-</sup> complex presumably gave rise to the active catalyst, which underwent oxidative insertion. Conversely, in the presence of a strong yet sterically hindered base such as NaOt-Bu (entry 7), the reaction was completely suppressed with no product formation observed, highlighting the need for a more coordinating base for the reaction to proceed efficiently.<sup>14</sup>

Several solvents proved to be tolerated in this reaction with high conversion also achieved with toluene and DMF (entries 3 and 8, respectively). However, *tert*-amyl alcohol proved to be optimal and furnished the rearranged product with complete conversion in the most consistent manner (entry 9). In the absence of palladium, the reaction did not proceed and complete recovery of  $\delta$ -lactam **5** was observed (entry 10).

Having established optimized conditions for the rearrangement of *N*-benzylactam **5**, we evaluated the applicability of the transformation using different substituted  $\delta$ -lactams, as well as *oxo*-lactams and *aza*-lactams. As illustrated in Table 2, different *N*-alkyl substituents were tolerated, and *N*-benzylactam **6** and *N*-methylactam **7** were isolated in 82 and 75% yields, respectively. Substitution at the lactam nitrogen was not required for the Pd(0)-catalyzed ring expansion reaction to proceed smoothly, as exemplified by the synthesis of NH-lactam **8** in 65% isolated yield. *N*-arylated substrates possessing a broad range of electronic properties also gave rise to the rearranged caprolactam

Table 2. Scope of Substituted *oxo*- and *aza*-Lactams<sup>a</sup>


<b>6</b>	82%
<b>7</b>	75%
<b>8</b>	65%
<b>9</b>	74%
<b>10</b>	74% <sup>b</sup>
<b>11</b>	>95%
<b>12</b>	73%
<b>13</b>	56%
<b>14</b>	0%

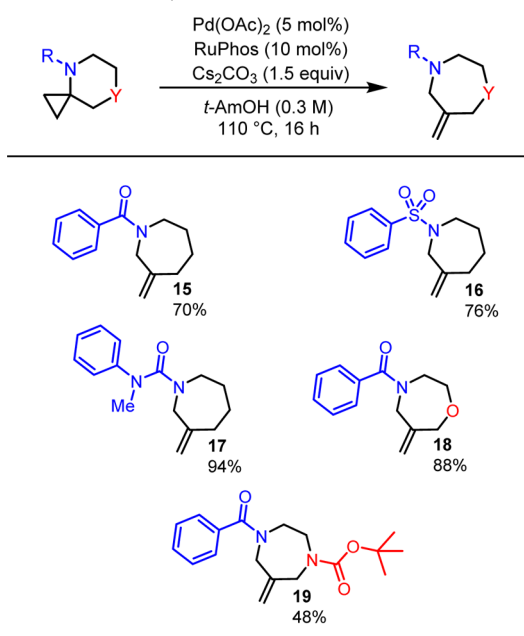
<sup>a</sup>All reactions were performed on 40 mg scale. <sup>b</sup>Reaction ran for 20 min.

products in good to excellent yields. For example, both *N*-phenyllactam **9** and electron-poor *N*-(4-nitrophenyl)lactam **10** were obtained in 74%, and electron-rich *N*-(4-dimethylaminophenyl)lactam **11** was isolated in 99% yield. Furthermore, *oxo*-lactam **12** was also compatible with the reaction conditions and was delivered in 73% yield. Similarly, a Boc-protected *aza*-lactam successfully provided desired heterocyclic product **13** in 56%. However, basic amines were not tolerated, and *N*-benzyl-*aza*-lactam **14** was not formed under the reaction conditions.

*N*-Substituted piperidines also proved to be efficient substrates for the Pd(0)-catalyzed rearrangement reaction (Table 3). For example, *N*-benzoylpiperidine was effectively converted to the corresponding azepane **15** in 70% yield. Sulfonamide and urea functionalities were also compatible and resulted in the formation of products **16** and **17** in 76 and 94% yields, respectively. Lastly, homomorpholine **18** and homopiperazine **19** were successfully obtained from the corresponding morpholine and piperazine starting materials in 88 and 48% yields, respectively. Overall, a broad range of  $\delta$ -lactams and saturated *N*-heterocycles reacted to yield the rearranged products, and the only observed limitation was the incompatibility of basic amines. It can therefore be inferred that the highly Lewis basic nature of these systems inhibited the catalyst by occupying an open coordination site required for the reaction to proceed, rendering it inactive toward the desired transformation.<sup>15</sup>

**Mechanistic Studies.** There is limited available information pertaining to the mechanism of the palladium-catalyzed C–C bond cleavage of unactivated cyclopropanes. Quantum mechanical studies reported by Blomberg<sup>16</sup> revealed that the C–C bond of unsubstituted cyclopropane was easier to break when compared to ethane and cyclobutane. This was due to a

**Table 3. Scope of *N*-Substituted Azepanes and Other Saturated *N*-Heterocycles<sup>a</sup>**



<sup>a</sup>All reactions were performed on 40 mg scale.

low activation barrier for the elimination reaction of metalacyclobutane, which in turn led to a small energy barrier for the reverse C–C bond oxidative addition process rather than depending strictly on the innate C–C bond strength.

Activated methylenecyclopropane C–C bond cleavage was also studied in the context of trimethylenemethane cycloaddition reactions.<sup>17</sup> The mechanism proposed by Trost<sup>18</sup> does not invoke palladium-mediated C–C bond oxidative addition. Conversely, Binger<sup>19</sup> proposed a mechanism including a palladacyclobutane intermediate. Subsequent theoretical studies by Fujimoto<sup>20</sup> supported the involvement of a palladacyclobutane intermediate, but no unifying mechanism had yet been established. Yamamoto<sup>21</sup> also demonstrated that methylenecyclopropanes may undergo ring opening via a palladium-catalyzed C–C bond oxidative addition to form palladacyclobutane intermediates in the presence of carbon-based nucleophiles. However, in the presence of nitrogen nucleophiles, C–C bond cleavage was proposed to proceed through  $\beta$ -carbon elimination.<sup>22</sup> More recently, Fu<sup>9</sup> reported the Pd(0)-catalyzed C–C bond cleavage of electronically activated 1,1-difluoro-2-arylcyclopropanes. Preliminary DFT calculations demonstrated that initial oxidative addition of a cyclopropane C–C bond to form a palladacyclobutane intermediate followed by  $\beta$ -fluorine elimination (Figure 1A, path B) was lower in energy than an initial C–F oxidative addition followed by  $\beta$ -carbon elimination (Figure 1A, Path A).

Similarly, we applied computational methods to investigate the two proposed mechanistic pathways for the cyclopropane ring expansion reaction of lactam **20** illustrated in Figure 2. All calculations were performed using DFT with the B3LYP density functional. The LANL2DZ basis set with the Hay–Wadt effective core potential was used for the Pd atom.<sup>23</sup> For all other atoms, the 6-31\* basis set was used. All stationary points were confirmed to be minima or transition states by computing the frequencies on optimized structures.<sup>24</sup>

Because of the more extensive computational power required for large systems, few reported all-atom DFT studies have been performed using the full structure of biarylphosphine

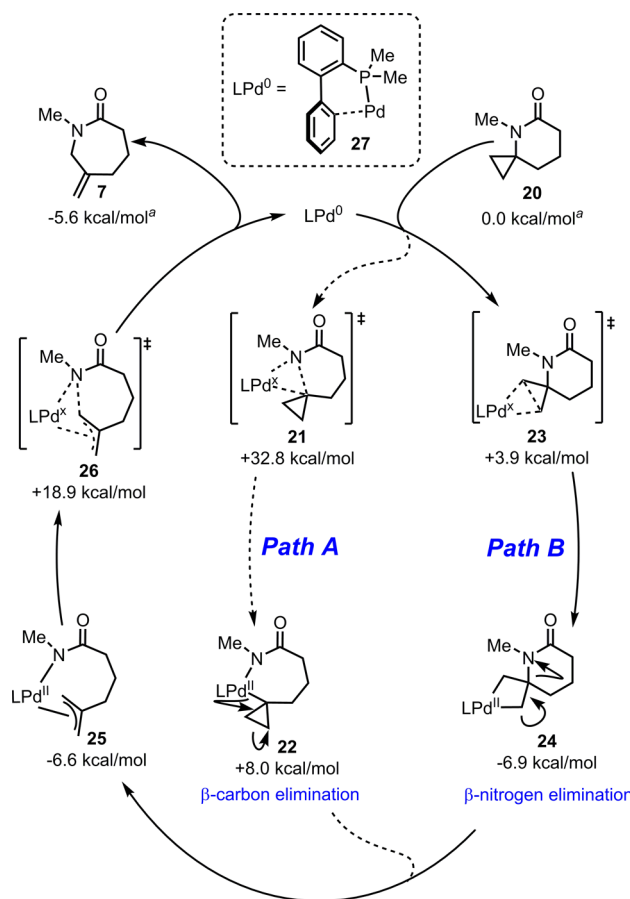


**Figure 2.** Computationally calculated mechanistic pathways for the rearrangement of piperidone **20** to caprolactam **7**. (a) Energies are reported as the sum of the energy of the separated compounds **20** or **7** and catalyst **27**.

ligands,<sup>25</sup> such as RuPhos,<sup>26</sup> which performed best in our reaction. However, it has been shown that potentially significant differences in calculated energies may occur when approximating the structure of ligands.<sup>27</sup> With this consideration in mind, we decided to elect biphenyldimethylphosphine (see Figure 2, complex **27**) as our model ligand for further DFT studies. We conducted initial optimization on the active monoligated LPd(0) catalyst.<sup>28</sup> The lowest energy conformation of the catalyst displayed an  $\eta^1$  interaction between the biphenyl substituent of the ligand and the palladium(0) center. We then performed geometry optimizations to identify low energy conformations of oxidative addition products **22** and **24** on the two pathways shown in Figure 2.<sup>29</sup> Optimizations were initiated from multiple input geometries to identify the lowest energy conformations.<sup>24</sup> The corresponding transition states **21** and **23** were identified using the QST2 method<sup>30</sup> in Gaussian.<sup>31</sup> The oxidative addition of the C–N bond of lactam **20** (Figure 2, path A) to palladium catalyst **27** was computed to present a transition state energy barrier of +32.8 kcal/mol (TS **21**), yielding palladacycle **22** at +8 kcal/mol. Conversely, it was revealed that the addition of the distal C–C bond of the cyclopropane ring (Figure 2, path B) had a much lower transition state energy of +3.9 kcal/mol (TS **23**), giving rise to palladacyclobutane **24** at –6.9 kcal/mol. On the basis of these results, it was concluded that path B, which involved the formation of a palladacyclobutane intermediate, was the operative reaction mechanism.<sup>32</sup>

It was hypothesized that the relief of the cyclopropane ring strain was the driving force that allowed for the low activation

energy barrier at the C–C bond cleavage step in TS 23 and the generation of energetically downhill palladacyclobutane intermediate 24. In contrast, the high energy barrier associated with the formation of palladacycle 22 in path A was hypothesized to be the result of a more sterically encumbered C–N bond precluding the approach of the active palladium center during the oxidative addition step. Additionally, intermediate 22 did not benefit from the relief of cyclopropane ring strain.

Both palladacycle intermediates 22 and 24 could then converge to common  $\pi$ -allyl complex 25 via a  $\beta$ -carbon elimination (Figure 2, path A) or a  $\beta$ -nitrogen elimination (Figure 2, path B), respectively. It was calculated that  $\pi$ -allyl intermediate 25 possessed an energy of  $-6.6$  kcal, similar to palladacyclobutane 24. Subsequent reductive elimination via TS 26 was judged to be rate-determining with an energy barrier of  $+18.9$  kcal/mol leading to product 7 ( $-5.6$  kcal/mol).<sup>33</sup>

To further analyze our proposed mechanism, we attempted to experimentally trap the various palladacycle intermediates under hydrogenative conditions and isolate the hydrogenated adducts for characterization (Figure 3). Treatment of lactam 28

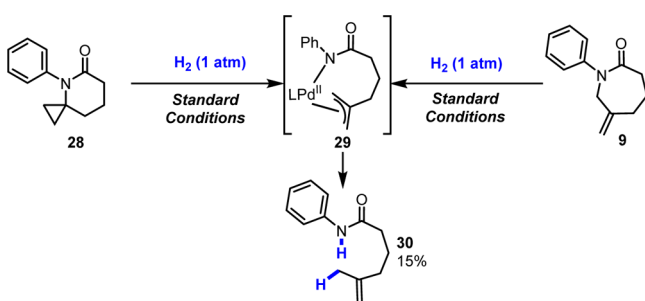


**Figure 3.** Treatment of lactams 28 and 9 under hydrogenation conditions.

under our optimized reaction conditions, with the addition of 1 atm of hydrogen, resulted in the formation of hydrogenated adduct 30 in 15% isolated yield. Other isolated products were the ring expanded product (9, 45% yield) and the hydrogenated olefin product (49, 35% yield, see Scheme 6). It was hypothesized that the formation of acyclic amide 30 was the product of homogeneous hydrogenation of  $\pi$ -allyl complex 29. This result confirmed the presence of this key  $\pi$ -allyl intermediate in the reaction mixture. Additionally, subjecting caprolactam 9 to the same reductive reaction conditions gave rise to the same amount of hydrogenated product (30). The generation of 30 from both cyclopropylpiperidone 28 and caprolactam 9 demonstrated that all reaction intermediates and products were in equilibrium under the reaction conditions. This was in agreement with the computed rate-determining energy barrier relative to the penultimate  $\pi$ -allyl intermediate ( $-6.6$  kcal/mol) and the final product ( $-5.6$  kcal/mol) energies. Interestingly, we did not observe a gem-dimethyl product, which would have resulted from the homogeneous hydrogenation of the calculated low-energy palladacyclobutane intermediate. Because both the palladacyclobutane (not shown) and the  $\pi$ -allyl complex (29) were calculated to possess similar ground state energies ( $-6.9$  and  $-6.6$  kcal/mol, respectively), it was hypothesized that both species should also be in equilibrium and in at a similar concentration in the reaction mixture. By applying the Curtin–Hammett principle,<sup>34</sup> it can be inferred that the corresponding barrier that produced hydrogenated amide product 30 from  $\pi$ -allyl complex 29 was lower in energy than the energy

barrier that would lead to a gem-dimethyl product from the calculated palladacyclobutane intermediate. As such, only 30 formed in the reaction mixture.

## CONCLUSIONS

In conclusion, we established Pd(0)-catalyzed conditions for the ring opening of spirocyclopropanes that led to the formation of functionalized caprolactams and azepanes in good to excellent yields. Mechanistic studies uncovered a low-energy palladacyclobutane intermediate that was energetically favored due to the relief of ring strain as a driving force. This represents the first Pd(0)-catalyzed C–C bond cleavage reaction of a spirocyclic cyclopropane that led to functionalized medium-sized nitrogen-containing heterocycles. In addition to its synthetic utility, this process also demonstrated the viability of cyclopropanes as reactive coupling partners in transition-metal-catalyzed synthetic transformations.

## EXPERIMENTAL SECTION

**General Information.** Reaction mixtures were analyzed on a UPLC-MS system using formic acid/MeCN mobile phases and a C18 column (1.7  $\mu$ m, 2.1  $\times$  30 mm). <sup>1</sup>H and <sup>13</sup>C NMR spectra were recorded in CDCl<sub>3</sub> solutions at 400 MHz for <sup>1</sup>H and 101 MHz for <sup>13</sup>C. The internal standard is TMS (0.00 ppm) for the resonance of protons and residual chloroform (77.0 ppm) for the resonance of carbons. High resolution mass spectra were obtained by positive EI and orbitrap mass analysis. Flash column chromatography purification was performed using disposable normal-phase 15–40  $\mu$ m silica gel columns. All reaction solvents were purchased anhydrous from commercial sources and used as is. The following compounds were purchased from commercial sources and were used as is 31 [546114-04-9], 32 [1100753-07-8], 33 [1199794-51-8], 39 [1199794-52-9], 41 [1301739-56-9], 42 [218595-22-3], 43 [886766-28-5].<sup>35</sup>

**General Procedure for Tables 2 and 3: Ring Expansion Reactions.** A sealable reaction vial was charged with the spirocyclopropane starting material (40 mg), palladium(II) acetate (0.05 equiv), RuPhos (0.10 equiv), and cesium carbonate (1.5 equiv) and then evacuated under vacuum and backfilled with argon (3 $\times$ ). *tert*-Amyl alcohol (0.3M) was added, and the resulting suspension was stirred and heated at 110  $^{\circ}$ C for 16 h. The reaction was then washed with CH<sub>2</sub>Cl<sub>2</sub> (3  $\times$  5 mL) and filtered through a pad of Celite. Concentrating the resulting filtrate followed by silica gel column chromatography (0–60% acetone in heptane) afforded the corresponding caprolactam or azepane product.

**1-Benzyl-6-methylene-azepan-2-one (6).** Yield: 33 mg, 82%; colorless oil; <sup>1</sup>H NMR (400 MHz, CDCl<sub>3</sub>)  $\delta$  7.27 (m, 5H), 4.81 (s, 1H), 4.62 (m, 3H), 3.72 (s, 2H), 2.69 (m, 2H), 2.36 (t,  $J$  = 6.0 Hz, 2H), 1.83 (m, 2H); <sup>13</sup>C NMR (101 MHz, CDCl<sub>3</sub>)  $\delta$  174.8, 143.3, 137.5, 128.5, 128.2, 127.3, 113.9, 53.2, 50.1, 37.0, 36.1, 24.0; HRMS calcd for C<sub>14</sub>H<sub>17</sub>NO [M + H]<sup>+</sup> 216.1383, found 216.1391.

**1-Methyl-6-methylene-azepan-2-one (7).** Yield: 30 mg, 75%; colorless oil; <sup>1</sup>H NMR (400 MHz, CDCl<sub>3</sub>)  $\delta$  4.88 (m, 2H), 3.80 (d,  $J$  = 0.7 Hz, 2H), 2.99 (s, 3H), 2.61 (m, 2H), 2.37 (m, 2H), 1.78 (m, 2H); <sup>13</sup>C NMR (101 MHz, CDCl<sub>3</sub>)  $\delta$  174.7, 143.4, 113.6, 56.0, 36.9, 35.8, 34.8, 24.0; HRMS calcd for C<sub>8</sub>H<sub>13</sub>NO [M + H]<sup>+</sup> 140.1070, found 140.1075.

**6-Methyleneazepan-2-one (8).** Yield: 26 mg, 65%; colorless oil; <sup>1</sup>H NMR (400 MHz, CDCl<sub>3</sub>)  $\delta$  6.28 (s, 1H), 4.88 (d,  $J$  = 12 Hz, 2H), 3.67 (d,  $J$  = 6.3 Hz, 2H), 2.54 (m, 2H), 2.42 (m, 2H), 1.79 (m, 2H); <sup>13</sup>C NMR (101 MHz, CDCl<sub>3</sub>)  $\delta$  177.6, 144.4, 114.0, 47.7, 37.4, 35.5, 23.5; HRMS calcd for C<sub>7</sub>H<sub>11</sub>NO [M + H]<sup>+</sup> 126.0914, found 126.0913.

**6-Methylene-1-phenyl-azepan-2-one (9).** Yield: 29.5 mg, 74%; colorless oil; <sup>1</sup>H NMR (400 MHz, CDCl<sub>3</sub>)  $\delta$  7.36 (m, 2H), 7.22 (m, 3H), 4.96 (s, 1H), 4.83 (s, 1H), 4.20 (s, 2H), 2.78 (m, 2H), 2.49 (m, 2H), 1.92 (m, 2H); <sup>13</sup>C NMR (101 MHz, CDCl<sub>3</sub>)  $\delta$  174.3, 144.0, 143.8, 129.1, 126.7, 126.6, 114.2, 57.5, 36.7, 36.4, 23.7; HRMS calcd for C<sub>13</sub>H<sub>15</sub>NO [M + H]<sup>+</sup> 202.1227, found 202.1233.



**6-Methylene-1-(4-nitrophenyl)azepan-2-one (10).** Reaction was run for 20 min instead of 16 h. Yield: 29.5 mg, 74%; colorless oil;  $^1\text{H}$  NMR (400 MHz,  $\text{CDCl}_3$ )  $\delta$  8.23 (d,  $J = 9.1$  Hz, 2H), 7.44 (d,  $J = 8.9$  Hz, 2H), 5.07–5.01 (m, 1H), 4.95–4.88 (m, 1H), 4.29 (s, 2H), 2.86–2.77 (m, 2H), 2.51 (td,  $J = 6.2, 1.1$  Hz, 2H), 2.01–1.86 (m, 2H);  $^{13}\text{C}$  NMR (101 MHz,  $\text{CDCl}_3$ )  $\delta$  174.2, 149.4, 145.4, 143.2, 126.7, 124.4, 114.7, 57.0, 36.4, 36.2, 23.3; HRMS calcd for  $\text{C}_{13}\text{H}_{14}\text{N}_2\text{O}_3$   $[\text{M} + \text{H}]^+$  247.1077, found 247.1093.

**1-(4-(Dimethylamino)phenyl)-6-methyleneazepan-2-one (11).** Yield: 39.5 mg, >95%; colorless oil;  $^1\text{H}$  NMR (400 MHz,  $\text{CDCl}_3$ )  $\delta$  7.10–6.97 (m, 2H), 6.78–6.63 (m, 2H), 4.98–4.90 (m, 1H), 4.87–4.79 (m, 1H), 4.15 (s, 2H), 2.94 (s, 6H), 2.80–2.71 (m, 2H), 2.52–2.44 (m, 2H), 1.97–1.85 (m, 2H);  $^{13}\text{C}$  NMR (101 MHz,  $\text{CDCl}_3$ )  $\delta$  174.6, 149.3, 144.0, 133.5, 127.1, 113.9, 112.9, 57.9, 40.7, 36.9, 36.4, 23.8; HRMS calcd for  $\text{C}_{15}\text{H}_{20}\text{N}_2\text{O}$   $[\text{M} + \text{H}]^+$  245.1648, found 245.1667.

**4-Benzyl-6-methylene-1,4-oxazepan-3-one (12).** Yield: 29 mg, 73%; colorless oil;  $^1\text{H}$  NMR (400 MHz,  $\text{CDCl}_3$ )  $\delta$  7.29 (m, 5H), 5.07 (s, 1H), 4.93 (s, 1H), 4.66 (s, 2H), 4.32 (s, 2H), 4.23 (s, 2H), 3.85 (s, 2H);  $^{13}\text{C}$  NMR (101 MHz,  $\text{CDCl}_3$ )  $\delta$  171.0, 143.0, 136.7, 128.6, 128.1, 127.5, 116.3, 73.7, 71.8, 51.6, 50.5; HRMS calcd for  $\text{C}_{13}\text{H}_{15}\text{NO}_2$   $[\text{M} + \text{H}]^+$  218.1176, found 218.1182.

**tert-Butyl 4-Isopropyl-6-methylene-3-oxo-1,4-diazepane-1-carboxylate (13).** Yield: 22.5 mg, 56%; colorless oil;  $^1\text{H}$  NMR (400 MHz,  $\text{CDCl}_3$ )  $\delta$  5.15 (m, 2H), 4.86 (m, 1H), 4.13 (m, 4H), 3.66 (m, 2H), 1.46 (s, 9H), 1.13 (d,  $J = 6.7$  Hz, 6H);  $^{13}\text{C}$  NMR (101 MHz,  $\text{CDCl}_3$ )  $\delta$  168.7, 155.2, 142.3, 116.3, 80.8, 52.1, 51.4, 45.5, 44.9, 28.2, 19.6; HRMS calcd for  $\text{C}_{14}\text{H}_{24}\text{N}_2\text{O}_3$   $[\text{M} + \text{H}]^+$  269.1860, found 269.1867.

**(3-Methyleneazepan-1-yl)(phenyl)methanone (15).** Yield: 28 mg, 70%; colorless oil;  $^1\text{H}$  NMR (400 MHz,  $\text{CDCl}_3$ , reported as a 2:1 mixture of rotamers)  $\delta$  7.46–7.31 (m, 5H), 5.00 (d,  $J = 11.3$  Hz, 2/3H), 4.86 (s, 2/3H), 4.78–4.66 (m, 2/3H), 4.34 (s, 2/3H), 4.02 (s, 4/3H), 3.67–3.56 (m, 4/3H), 3.38–3.24 (m, 2/3H), 2.41–2.29 (m, 2/3H), 2.28–2.17 (m, 4/3H), 1.91–1.77 (m, 4/3H), 1.75–1.59 (m, 2H), 1.59–1.48 (m, 2/3H);  $^{13}\text{C}$  NMR (101 MHz,  $\text{CDCl}_3$ , reported as a mixture of rotamers)  $\delta$  172.0, 171.1, 147.6, 146.4, 137.0, 136.7, 129.2, 129.1, 128.3, 126.7, 126.4, 114.0, 112.3, 56.8, 52.6, 49.0, 46.5, 34.9, 34.6, 30.6, 29.8, 28.3, 28.2; HRMS calcd for  $\text{C}_{14}\text{H}_{17}\text{NO}$   $[\text{M} + \text{H}]^+$  216.1383, found 216.1388.

**3-Methylene-1-(phenylsulfonyl)azepane (16).** Yield: 30.5 mg, 76%; colorless oil;  $^1\text{H}$  NMR (400 MHz,  $\text{CDCl}_3$ )  $\delta$  7.84–7.78 (m, 2H), 7.61–7.47 (m, 3H), 4.90–4.86 (m, 1H), 4.84–4.81 (m, 1H), 3.94–3.87 (m, 2H), 3.23–3.16 (m, 2H), 2.32–2.24 (m, 2H), 1.79–1.69 (m, 2H), 1.64–1.53 (m, 2H);  $^{13}\text{C}$  NMR (101 MHz,  $\text{CDCl}_3$ )  $\delta$  146.8, 139.4, 132.3, 129.0, 126.9, 113.2, 54.6, 48.1, 34.0, 30.5, 29.3; HRMS calcd for  $\text{C}_{13}\text{H}_{17}\text{NO}_2\text{S}$   $[\text{M} + \text{H}]^+$  252.1053, found 252.1058.

**N-Methyl-3-methylene-N-phenylazepane-1-carboxamide (17).** Yield: 37.5 mg, 94%; colorless oil;  $^1\text{H}$  NMR (400 MHz,  $\text{CDCl}_3$ )  $\delta$  7.38–7.28 (m, 2H), 7.17–7.00 (m, 3H), 4.76 (d,  $J = 1.9$  Hz, 1H), 4.70–4.62 (m, 1H), 3.65 (s, 2H), 3.26–3.12 (m, 5H), 2.24–2.07 (m, 2H), 1.67–1.57 (m, 2H), 1.57–1.48 (m, 2H);  $^{13}\text{C}$  NMR (101 MHz,  $\text{CDCl}_3$ )  $\delta$  161.8, 148.2, 147.2, 129.4, 124.3, 123.8, 112.3, 55.5, 48.0, 40.0, 34.4, 29.4, 28.6; HRMS calcd for  $\text{C}_{13}\text{H}_{20}\text{N}_2\text{O}$   $[\text{M} + \text{H}]^+$  245.1649, found 245.1658.

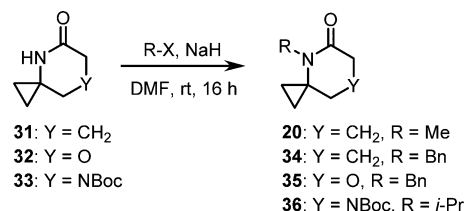
**N-Methyl-3-methylene-N-phenylazepane-1-carboxamide (18).** Yield: 35 mg, 88%; colorless oil;  $^1\text{H}$  NMR (400 MHz,  $\text{CDCl}_3$ , reported as a 2:1 mixture of rotamers)  $\delta$  7.47–7.33 (m, 5H), 5.27 (br s, 1/3H), 5.11 (br s, 1/3H), 4.99 (br s, 2/3H), 4.72 (br s, 2/3H), 4.42 (br s, 2/3H), 4.29 (br s, 2/3H), 4.24 (br s, 4/3H), 4.11 (br s, 4/3H), 3.88 (br s, 2/3H), 3.64 (br s, 2/3H), 3.52 (br s, 2/3H);  $^{13}\text{C}$  NMR (101 MHz,  $\text{CDCl}_3$ , reported as a mixture of rotamers)  $\delta$  166.8, 140.6, 139.3, 131.5, 131.2, 124.9, 124.8, 123.8, 123.6, 122.0, 121.8, 109.9, 108.4, 69.8, 69.6, 67.8, 50.1, 47.9, 45.5, 44.9; HRMS calcd for  $\text{C}_{13}\text{H}_{16}\text{NO}_2$   $[\text{M} + \text{H}]^+$  218.1176, found 218.1179.

**N-Methyl-3-methylene-N-phenylazepane-1-carboxamide (19).** Yield: 19 mg, 48%; colorless oil;  $^1\text{H}$  NMR (400 MHz,  $\text{CDCl}_3$ , reported as a mixture of rotamers)  $\delta$  7.49–7.29 (m, 5H), 5.38–4.47 (m, 2H), 4.29–3.79 (m, 5H), 3.71–3.25 (m, 3H), 1.46 (s, 9H);  $^{13}\text{C}$  NMR (101 MHz,  $\text{CDCl}_3$ , reported as a mixture of rotamers)  $\delta$  167.2,

167.1, 166.7, 150.3, 150.0, 139.6, 139.3, 138.3, 137.9, 137.4, 131.4, 131.3, 124.8, 123.8, 123.5, 121.9, 121.7, 110.2, 108.6, 107.1, 75.4, 75.3, 50.5, 48.0, 47.7, 47.0, 46.4, 46.1, 45.5, 44.9, 44.4, 44.0, 43.9, 43.5, 23.6; HRMS calcd for  $\text{C}_{18}\text{H}_{25}\text{N}_2\text{O}_3$   $[\text{M} + \text{H}]^+$  317.1860, found 317.1863.

**8-Methyl-8-azaspiro[2.5]octan-7-one (20) (Scheme 1).** A round-bottomed flask was charged with 8-azaspiro[2.5]octan-7-one (200 mg,

### Scheme 1. Preparation of Starting Materials 20 and 34-36



1.60 mmol) and *N,N*-dimethylformamide (5.3 mL). The resulting solution was cooled to 0 °C, and sodium hydride (60% in mineral oil, 51 mg, 1.3 mmol) was added, forming a yellow suspension. The suspension was then allowed to warm to room temperature, and iodomethane (0.13 mL, 2.1 mmol) was added. The reaction mixture was stirred for 16 h. Upon completion, the reaction was quenched with  $\text{H}_2\text{O}$  (1 mL), extracted with ethyl acetate (3 × 3 mL), and dried with anhydrous  $\text{MgSO}_4$ . Concentrating the organic layer followed by silica gel column chromatography (0–60% acetone in heptane) afforded 8-methyl-8-azaspiro[2.5]octan-7-one (64.5 mg, 29% yield) as a colorless gel.  $^1\text{H}$  NMR (400 MHz,  $\text{CDCl}_3$ )  $\delta$  2.70 (s, 3H), 2.51 (d,  $J = 6.0$  Hz, 2H), 1.86 (m, 2H), 1.69 (m, 2H), 1.01 (d,  $J = 6.0$  Hz, 2H), 0.58 (m, 2H);  $^{13}\text{C}$  NMR (101 MHz,  $\text{CDCl}_3$ )  $\delta$  172.3, 40.3, 33.3, 32.2, 27.5, 19.3, 9.8; HRMS calcd for  $\text{C}_8\text{H}_{13}\text{NO}$   $[\text{M} + \text{H}]^+$  140.1070, found 140.1070.

**8-Benzyl-8-azaspiro[2.5]octan-7-one (34) (Scheme 1).** A round-bottomed flask was charged with 8-azaspiro[2.5]octan-7-one (200 mg, 1.60 mmol) and *N,N*-dimethylformamide (5.3 mL). The resulting solution was cooled to 0 °C, and sodium hydride (60% in mineral oil, 51 mg, 1.3 mmol) was added, forming a yellow suspension. The suspension was then allowed to warm to room temperature, and benzyl bromide (0.25 mL, 2.1 mmol) was added. The reaction mixture was stirred for 16 h. Upon completion, the reaction was quenched with  $\text{H}_2\text{O}$  (1 mL), extracted with ethyl acetate (3 × 3 mL), and dried with anhydrous  $\text{MgSO}_4$ . Concentrating the organic layer followed by silica gel column chromatography (0–60% acetone in heptane) afforded 8-benzyl-8-azaspiro[2.5]octan-7-one (26.5 mg, 77% yield) as a white amorphous solid.  $^1\text{H}$  NMR (400 MHz,  $\text{CDCl}_3$ )  $\delta$  7.35–7.09 (m, 5H), 4.46 (s, 2H), 2.63 (t,  $J = 7.1$  Hz, 2H), 1.93 (p,  $J = 6.9$  Hz, 2H), 1.63 (t,  $J = 6.8$  Hz, 2H), 0.93–0.85 (m, 2H), 0.60–0.52 (m, 2H);  $^{13}\text{C}$  NMR (101 MHz,  $\text{CDCl}_3$ )  $\delta$  173.3, 138.7, 128.5, 126.8, 126.7, 44.8, 39.9, 33.4, 32.2, 19.3, 11.2; HRMS calcd for  $\text{C}_{14}\text{H}_{17}\text{NO}$   $[\text{M} + \text{H}]^+$  216.1383, found 216.1388.

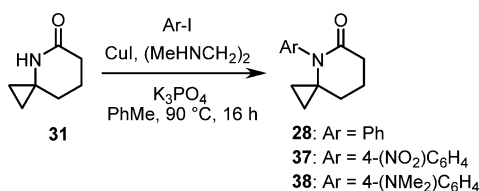
**8-Benzyl-5-oxa-8-azaspiro[2.5]octan-7-one (35) (Scheme 1).** A round-bottomed flask was charged with 5-oxa-8-azaspiro[2.5]octan-7-one (200 mg, 1.57 mmol) and *N,N*-dimethylformamide (3.2 mL). The resulting solution was cooled to 0 °C, and sodium hydride (60% in mineral oil, 47 mg, 1.2 mmol) was added, forming a yellow suspension. The suspension was then allowed to warm to room temperature, and benzyl bromide (0.24 mL, 2.0 mmol) was added. The reaction mixture was stirred for 16 h. Upon completion, the reaction was quenched with  $\text{H}_2\text{O}$  (1 mL), extracted with ethyl acetate (3 × 3 mL), and dried with anhydrous  $\text{MgSO}_4$ . Concentrating the organic layer followed by silica gel column chromatography (0–60% acetone in heptane) afforded 8-benzyl-8-azaspiro[2.5]octan-7-one (177 mg, 52% yield) as a white amorphous solid.  $^1\text{H}$  NMR (400 MHz,  $\text{CDCl}_3$ )  $\delta$  7.36–7.27 (m, 2H), 7.27–7.21 (m, 1H), 7.19 (dd,  $J = 7.5, 1.7$  Hz, 2H), 4.45 (s, 2H), 4.43 (s, 2H), 3.69 (s, 2H), 1.02–0.95 (m, 2H), 0.71–0.65 (m, 2H);  $^{13}\text{C}$  NMR (101 MHz,  $\text{CDCl}_3$ )  $\delta$  168.5, 137.6, 128.7, 127.2, 126.4, 72.5, 68.2, 43.1, 39.0, 7.8; HRMS calcd for  $\text{C}_{13}\text{H}_{15}\text{NO}_2$   $[\text{M} + \text{H}]^+$  218.1176, found 218.1185.

**tert-Butyl 8-Isopropyl-7-oxo-5,8-diazaspiro[2.5]octane-5-carboxylate (36) (Scheme 1).** A round-bottomed flask was charged with *tert*-butyl 7-oxo-5,8-diazaspiro[2.5]octane-5-carboxylate (200 mg, 0.88 mmol)

and *N,N*-dimethylformamide (2.9 mL). The resulting solution was cooled to 0 °C, and sodium hydride (60% in mineral oil, 53 mg, 1.3 mmol) was added, forming a yellow suspension. The suspension was then allowed to warm to room temperature, and 2-iodopropane (0.26 mL, 2.7 mmol) was added. The reaction mixture was stirred for 16 h. Upon completion, the reaction was quenched with H<sub>2</sub>O (1 mL), extracted with ethyl acetate (3 × 3 mL), and dried with anhydrous MgSO<sub>4</sub>. Concentrating the organic layer followed by silica gel column chromatography (0–60% acetone in heptane) afforded *tert*-butyl 8-isopropyl-7-oxo-5,8-diazaspiro[2.5]octane-5-carboxylate (85 mg, 36% yield) as a white amorphous solid. <sup>1</sup>H NMR (400 MHz, CDCl<sub>3</sub>) δ 4.20 (m, 3H), 3.23 (m, 2H), 1.46 (s, 9H), 1.26 (d, *J* = 7.0 Hz, 6H), 1.15 (d, *J* = 6.0 Hz, 2H), 0.92 (s, 2H); <sup>13</sup>C NMR (101 MHz, CDCl<sub>3</sub>, major rotamer reported) δ 170.1, 154.1, 80.3, 52.4, 49.0, 46.8, 37.1, 28.3, 20.8, 12.0; HRMS calcd for C<sub>14</sub>H<sub>24</sub>N<sub>2</sub>O<sub>3</sub> [M + H]<sup>+</sup> 269.1860, found 269.1870.

**8-Phenyl-8-azaspiro[2.5]octan-7-one (28)** (Scheme 2). A sealable reaction vial was charged with 8-azaspiro[2.5]octan-7-one (200 mg,

**Scheme 2. Preparation of Starting Materials 28, 37, and 38**



1.6 mmol), copper(I) iodide (30 mg, 0.154 mmol), and potassium phosphate (754 mg, 3.5 mmol) and then evacuated under vacuum and backfilled with argon (3×). Toluene (3.2 mL), *N,N*-dimethylethylenediamine (0.035 mL, 0.32 mmol), and iodobenzene (0.23 mL, 2.1 mmol) were then added, and the resulting slurry was heated at 90 °C and stirred for 16 h. The reaction was then quenched with H<sub>2</sub>O (1 mL), diluted with EtOAc (3 × 5 mL), washed with 1 M HCl, saturated aqueous NaHCO<sub>3</sub>, and brine, and dried with anhydrous MgSO<sub>4</sub>. Concentrating the organic layer followed by silica gel column chromatography (0–60% acetone in heptane) afforded 8-phenyl-8-azaspiro[2.5]octan-7-one (190 mg, 59% yield) as a white amorphous solid. <sup>1</sup>H NMR (400 MHz, CDCl<sub>3</sub>) δ 7.36 (m, 2H), 7.27 (m, 1H), 7.07 (m, 2H), 2.69 (d, *J* = 8.0 Hz, 2H), 2.03 (d, *J* = 7.0 Hz, 2H), 1.88 (d, *J* = 8.0 Hz, 2H), 0.64 (s, 4H); <sup>13</sup>C NMR (101 MHz, CDCl<sub>3</sub>) δ 172.7, 138.4, 128.9, 128.5, 127.2, 41.6, 33.1, 32.7, 19.4, 12.1; HRMS calcd for C<sub>13</sub>H<sub>15</sub>NO [M + H]<sup>+</sup> 202.1227, found 202.1231.

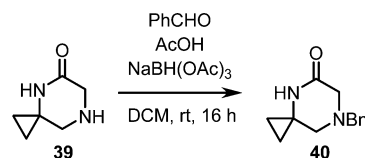
**8-(4-Nitrophenyl)-8-azaspiro[2.5]octan-7-one (37)** (Scheme 2). A sealable reaction vial was charged with 8-azaspiro[2.5]octan-7-one (200 mg, 1.6 mmol), copper(I) iodide (30 mg, 0.154 mmol), and potassium phosphate (754 mg, 3.5 mmol) and then evacuated under vacuum and backfilled with argon (3×). Toluene (3.2 mL), *N,N*-dimethylethylenediamine (0.035 mL, 0.32 mmol), and 1-iodo-4-nitrobenzene (522 mg, 2.1 mmol) were then added, and the resulting slurry was heated at 100 °C and stirred for 16 h. The reaction was then quenched with H<sub>2</sub>O (1 mL), diluted with EtOAc (3 × 5 mL), washed with 1 M HCl, saturated aqueous NaHCO<sub>3</sub>, and brine, and dried with anhydrous MgSO<sub>4</sub>. Concentrating the organic layer followed by silica gel column chromatography (0–60% acetone in heptane) afforded 8-(4-nitrophenyl)-8-azaspiro[2.5]octan-7-one (240 mg, 61% yield) as a white amorphous solid. <sup>1</sup>H NMR (400 MHz, CDCl<sub>3</sub>) δ 8.22 (d, *J* = 9.1 Hz, 2H), 7.36 (d, *J* = 9.1 Hz, 2H), 2.74 (t, *J* = 7.1 Hz, 2H), 2.14–2.03 (m, 2H), 1.98–1.88 (m, 2H), 0.91–0.83 (m, 2H), 0.74–0.66 (m, 2H); <sup>13</sup>C NMR (101 MHz, CDCl<sub>3</sub>) δ 173.4, 145.5, 144.7, 127.8, 124.1, 41.47, 32.9, 32.1, 19.0, 13.9; HRMS calcd for C<sub>13</sub>H<sub>14</sub>N<sub>2</sub>O<sub>3</sub> [M + H]<sup>+</sup> 247.1077, found 247.1093.

**8-(4-Dimethylaminophenyl)-8-azaspiro[2.5]octan-7-one (38)** (Scheme 2). A sealable reaction vial was charged with 8-azaspiro[2.5]octan-7-one (200 mg, 1.6 mmol), copper(I) iodide (30 mg, 0.154 mmol), and potassium phosphate (754 mg, 3.5 mmol) and then evacuated under vacuum and backfilled with argon (3×). Toluene (3.2 mL), *N,N*-dimethylethylenediamine (0.035 mL, 0.32 mmol), and 4-iodo-*N,N*-dimethylaniline (518 mg, 2.1 mmol) were then added, and the resulting

slurry was heated at 100 °C and stirred for 20 h. The reaction was then quenched with H<sub>2</sub>O (1 mL), diluted with EtOAc (3 × 5 mL), washed with saturated aqueous NaHCO<sub>3</sub> and brine, and dried with anhydrous MgSO<sub>4</sub>. Concentrating the organic layer followed by silica gel column chromatography (0–60% acetone in heptane) afforded 8-(4-dimethylaminophenyl)-8-azaspiro[2.5]octan-7-one (148.5 mg, 38% yield) as a yellow amorphous solid. <sup>1</sup>H NMR (400 MHz, CDCl<sub>3</sub>) δ 6.89 (d, *J* = 8.9 Hz, 2H), 6.68 (d, *J* = 8.9 Hz, 2H), 2.94 (s, 6H), 2.66 (t, *J* = 13.9 Hz, 2H), 2.05–1.96 (m, 2H), 1.88–1.81 (m, 2H), 0.66–0.60 (m, 2H), 0.60–0.53 (m, 2H); <sup>13</sup>C NMR (101 MHz, CDCl<sub>3</sub>) δ 172.7, 149.5, 129.2, 127.0, 112.6, 41.8, 40.6, 33.3, 32.7, 19.6, 11.4; HRMS calcd for C<sub>15</sub>H<sub>20</sub>N<sub>2</sub>O [M + H]<sup>+</sup> 245.1648, found 245.1660.

**5-Benzyl-5,8-diazaspiro[2.5]octan-7-one (40)** (Scheme 3). A round-bottomed flask was charged with 5,8-diazaspiro[2.5]octan-7-

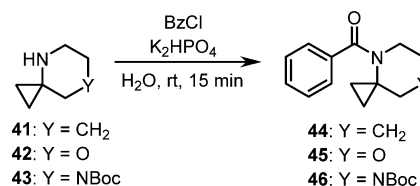
**Scheme 3. Preparation of Starting Material 40**



one hydrochloride (200 mg, 1.59 mmol) and dichloromethane (5.3 mL), and benzaldehyde (0.16 mL, 1.59 mmol) was added. Sodium triacetoxyborohydride (531 mg, 2.38 mmol) and acetic acid (0.14 mL, 2.38 mmol) were then added, and the reaction was allowed to stir at room temperature for 16 h. The reaction was then quenched with H<sub>2</sub>O (1 mL), diluted with EtOAc (3 × 5 mL), washed with 1 M HCl, saturated aqueous NaHCO<sub>3</sub>, and brine, and dried with anhydrous MgSO<sub>4</sub>. Concentrating the organic layer followed by silica gel column chromatography (0–60% acetone in heptane) afforded 5-benzyl-5,8-diazaspiro[2.5]octan-7-one (123.5 mg, 36% yield) as a white amorphous solid. <sup>1</sup>H NMR (400 MHz, CDCl<sub>3</sub>) δ 7.30 (m, 5H), 3.62 (s, 2H), 3.25 (s, 2H), 2.53 (s, 2H), 0.75 (m, 2H), 0.65 (m, 2H); <sup>13</sup>C NMR (101 MHz, CDCl<sub>3</sub>) δ 170.6, 137.1, 128.8, 128.4, 127.4, 61.1, 56.3, 56.1, 34.9, 11.7; HRMS calcd for C<sub>13</sub>H<sub>16</sub>N<sub>2</sub>O [M + H]<sup>+</sup> 217.1336, found 217.1345.

**Phenyl(4-azaspiro[2.5]octan-4-yl)methanone (44)** (Scheme 4). 8-Azaspiro[2.5]octane hydrochloride (0.450 g, 3.05 mmol) and potassium

**Scheme 4. Preparation of Starting Materials 44–46**



phosphate dibasic (0.5 M in H<sub>2</sub>O, 10 mL) were combined at room temperature. Benzoyl chloride (450 mg, 3.20 mmol) was added dropwise to the stirred solution. A precipitate formed as the reagent was added. The resulting slurry was stirred for 15 min at room temperature, and then CPME (6 mL) was added. The organic fraction was isolated, and the aqueous layer was rinsed with CPME (6 mL) a second time. The organic fractions were combined, dried over Na<sub>2</sub>SO<sub>4</sub>, filtered, and concentrated under reduced pressure. The resulting oil was purified by column chromatography (25% EtOAc in heptane) to yield phenyl(4-azaspiro[2.5]octan-4-yl)methanone as a white amorphous solid (510 mg, 74%). <sup>1</sup>H NMR (400 MHz, CDCl<sub>3</sub>) δ 7.50–7.30 (m, 5H), 3.53 (br s, 2H), 1.80 (br s, 2H), 1.61 (br s, 4H), 0.58 (br s, 4H); <sup>13</sup>C NMR (101 MHz, CDCl<sub>3</sub>, reported as mixture of rotamers) δ 171.8, 169.7, 137.4, 129.6, 128.1, 127.1, 49.9, 44.8, 39.9, 38.3, 35.3, 32.2, 26.5, 24.1, 14.8; HRMS calcd for C<sub>14</sub>H<sub>17</sub>NO [M + H]<sup>+</sup> 216.1383, found 216.1388.

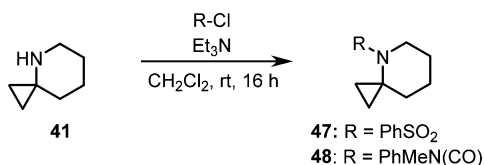
**Phenyl(7-oxa-4-azaspiro[2.5]octan-4-yl)methanone (45)** (Scheme 4). 8-Azaspiro[2.5]octane hydrochloride (0.50 g, 3.3 mmol) and potassium phosphate dibasic (0.5 M in H<sub>2</sub>O, 10 mL) were combined

at room temperature. Benzoyl chloride (0.43 mL, 3.7 mmol) was added dropwise to the stirred solution. A precipitate formed as the reagent was added. The resulting slurry was stirred for 15 min at room temperature, and then CPME (6 mL) was added. The organic fraction was isolated, and the aqueous layer was rinsed with CPME (6 mL) a second time. The organic fractions were combined, dried over  $\text{Na}_2\text{SO}_4$ , filtered, and concentrated under reduced pressure. The resulting oil was purified by column chromatography (25% EtOAc in heptane) to yield phenyl-(7-oxa-4-azaspiro[2.5]octan-4-yl)methanone as a white amorphous solid (466 mg, 58%).  $^1\text{H}$  NMR (400 MHz,  $\text{CDCl}_3$ )  $\delta$  7.52–7.31 (m, 5H), 3.88–3.67 (m, 4H), 3.61 (s, 2H), 0.97–0.73 (m, 4H);  $^{13}\text{C}$  NMR (101 MHz,  $\text{CDCl}_3$ , reported as mixture of rotamers)  $\delta$  170.9, 136.6, 130.2, 129.6, 128.5, 128.3, 127.5, 126.9, 73.6, 68.9, 67.3, 67.1, 48.1, 39.3, 13.6, 10.5; HRMS calcd for  $\text{C}_{13}\text{H}_{16}\text{NO}_2$  [ $\text{M} + \text{H}$ ] $^+$  218.1176, found 218.1179.

**tert-Butyl 4-benzoyl-4,7-diazaspiro[2.5]octane-7-carboxylate (46)** (Scheme 4). *tert*-Butyl 4,7-diazaspiro[2.5]octane-7-carboxylate (0.537 g, 2.5 mmol) and potassium phosphate dibasic (0.5 M in  $\text{H}_2\text{O}$ , 10 mL) were combined at room temperature. Benzoyl chloride (0.32 mL, 2.7 mmol) was added dropwise to the stirred solution. A precipitate formed as the reagent was added. The resulting slurry was stirred for 15 min at room temperature, and then CPME (6 mL) was added. The organic fraction was isolated, and the aqueous layer was rinsed with CPME (6 mL) a second time. The organic fractions were combined, dried over  $\text{Na}_2\text{SO}_4$ , filtered, and concentrated under reduced pressure. The resulting oil was purified by column chromatography (25% EtOAc in heptane) to yield *tert*-butyl 4-benzoyl-4,7-diazaspiro[2.5]octane-7-carboxylate as a white amorphous solid (720 mg, 91%).  $^1\text{H}$  NMR (400 MHz,  $\text{CDCl}_3$ )  $\delta$  7.51–7.29 (m, 5H), 3.77–3.60 (m, 2H), 3.54–3.45 (m, 2H), 3.43 (s, 2H), 1.46 (s, 9H), 0.90–0.72 (m, 4H);  $^{13}\text{C}$  NMR (101 MHz,  $\text{CDCl}_3$ , reported as a mixture of rotamers)  $\delta$  171.0, 154.8, 136.5, 133.0, 130.1, 129.9, 128.2, 127.3, 80.0, 67.5, 51.0, 46.9, 44.1, 38.7, 28.3, 21.7, 21.2, 14.1; HRMS calcd for  $\text{C}_{18}\text{H}_{25}\text{N}_2\text{O}_3$  [ $\text{M} + \text{H}$ ] $^+$  317.1860, found 317.1863.

**8-(Benzenesulfonyl)-8-azaspiro[2.5]octane (47)** (Scheme 5). To a solution of 4-azaspiro[2.5]octane hydrochloride (150 mg, 1.01 mmol)

#### Scheme 5. Preparation of Starting Materials 47 and 48

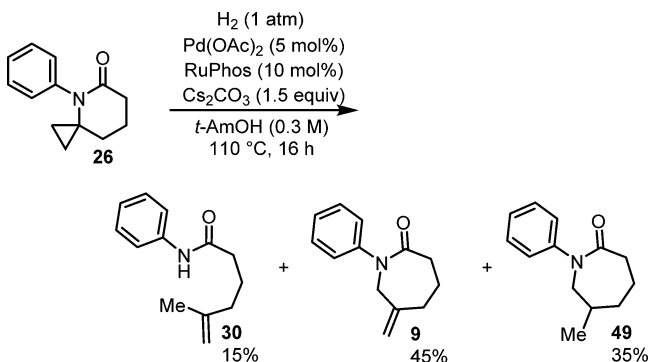


in dichloromethane (5 mL) was added triethylamine (0.43 mL, 3.04 mmol) and benzenesulfonyl chloride (0.19 mL, 1.52 mmol), and the reaction was stirred at room temperature for 16 h. The reaction was then concentrated on silica gel and purified by silica gel column chromatography (0–100% EtOAc in heptane) to give 8-(benzenesulfonyl)-8-azaspiro[2.5]octane (239 mg, 94% yield) as a white amorphous solid.  $^1\text{H}$  NMR (400 MHz,  $\text{CDCl}_3$ )  $\delta$  7.90–7.79 (m, 2H), 7.60–7.42 (m, 3H), 3.64–3.49 (m, 2H), 1.71–1.61 (m, 2H), 1.61–1.51 (m, 2H), 1.31–1.19 (m, 2H), 1.05–0.94 (m, 2H), 0.60–0.52 (m, 2H);  $^{13}\text{C}$  NMR (101 MHz,  $\text{CDCl}_3$ )  $\delta$  142.6, 132.2, 128.9, 127.1, 48.1, 39.3, 32.0, 24.3, 23.7, 13.9; HRMS calcd for  $\text{C}_{13}\text{H}_{17}\text{NO}_2\text{S}$  [ $\text{M} + \text{H}$ ] $^+$  252.1053, found 252.1064.

***N*-Methyl-*N*-phenyl-8-azaspiro[2.5]octane-8-carboxamide (48)** (Scheme 5). To a solution of 4-azaspiro[2.5]octane hydrochloride (150 mg, 1.01 mmol) in dichloromethane (5 mL) was added triethylamine (0.43 mL, 3.04 mmol) and *N*-methyl-*N*-phenylcarbamoyl chloride (258 mg, 1.52 mmol), and the reaction was stirred at room temperature for 16 h. The reaction was then concentrated on silica gel and purified by silica gel column chromatography (0–100% EtOAc in heptane) to give *N*-methyl-*N*-phenyl-8-azaspiro[2.5]octane-8-carboxamide (222 mg, 90% yield) as a white amorphous solid.  $^1\text{H}$  NMR (400 MHz,  $\text{CDCl}_3$ )  $\delta$  7.32–7.24 (m, 2H), 7.11–6.99 (m, 3H), 3.21 (s, 3H), 3.04–2.91 (m, 2H), 1.68–1.56 (m, 2H), 1.51–1.31 (m, 4H), 0.82–0.72 (m, 2H), 0.67–0.54 (m, 2H);  $^{13}\text{C}$  NMR (101 MHz,  $\text{CDCl}_3$ )  $\delta$  161.0, 146.7, 129.0, 124.3, 124.1, 48.1, 38.8, 38.7, 31.6, 26.0, 24.0, 14.7; HRMS calcd for  $\text{C}_{15}\text{H}_{20}\text{N}_2\text{O}$  [ $\text{M} + \text{H}$ ] $^+$  245.1649, found 245.1658.

Reaction of Piperidine 26 under Hydrogenation Conditions (Scheme 6). A sealable reaction vial was charged with 4-phenyl-4-

#### Scheme 6. Reaction of Piperidine 26 under Hydrogenation Conditions



azaspiro[2.5]octan-5-one (50 mg, 0.248 mmol), palladium(II) acetate (2.8 mg, 0.012 mmol), RuPhos (11.8 mg, 0.025 mmol), and cesium carbonate (121 mg, 0.37 mmol) and then evacuated under vacuum and backfilled with argon (3 $\times$ ). *tert*-Amyl alcohol (1 mL) was added, and the reaction mixture was evacuated under vacuum and backfilled with hydrogen (3 $\times$ ). A hydrogen-filled balloon was placed on top of the reaction vessel. The resulting suspension was heated at 110  $^\circ\text{C}$  and stirred for 16 h. The reaction was washed with  $\text{CH}_2\text{Cl}_2$  (3  $\times$  5 mL) and filtered through Celite. Concentrating the filtrate followed by silica gel column chromatography (0–60% acetone in heptane) afforded 5-methyl-*N*-phenylhex-5-enamide (7.5 mg, 15% yield) as a colorless oil, 6-methylene-1-phenylazepan-2-one (22.5 mg, 45% yield) as a colorless oil, and 6-methyl-1-phenylazepan-2-one (17.5 mg, 35% yield) as a colorless oil.

**5-Methyl-*N*-phenylhex-5-enamide (30)**.  $^1\text{H}$  NMR (400 MHz,  $\text{CDCl}_3$ )  $\delta$  7.56–7.46 (m, 2H), 7.36–7.29 (m, 2H), 7.13–7.07 (m, 1H), 4.77 (s, 1H), 4.72 (s, 1H), 2.41–2.29 (m, 2H), 2.12 (t,  $J = 7.5$  Hz, 2H), 1.96–1.84 (m, 2H), 1.74 (s, 3H), 1.61 (s, 1H);  $^{13}\text{C}$  NMR (101 MHz,  $\text{CDCl}_3$ , C=O carbon could not be differentiated from baseline)  $\delta$  144.9, 137.8, 129.0, 124.2, 119.6, 110.8, 37.0, 36.9, 23.1, 22.1; HRMS calcd for  $\text{C}_{13}\text{H}_{17}\text{NO}$  [ $\text{M} + \text{H}$ ] $^+$  204.1383, found 204.1388.

**6-Methyl-1-phenylazepan-2-one (49)**.  $^1\text{H}$  NMR (400 MHz,  $\text{CDCl}_3$ )  $\delta$  7.43–7.32 (m, 2H), 7.25–7.15 (m, 3H), 3.69 (dd,  $J = 15.0, 9.2$  Hz, 1H), 3.46 (dt,  $J = 15.0, 1.5$  Hz, 1H), 2.78–2.62 (m, 2H), 2.02–1.93 (m, 2H), 1.84–1.63 (m, 2H), 1.48–1.29 (m, 1H), 0.94 (d,  $J = 6.8$  Hz, 3H);  $^{13}\text{C}$  NMR (101 MHz,  $\text{CDCl}_3$ )  $\delta$  175.4, 144.7, 129.1, 126.4, 126.2, 59.1, 38.3, 37.5, 34.0, 22.7, 20.0; HRMS calcd for  $\text{C}_{13}\text{H}_{17}\text{NO}$  [ $\text{M} + \text{H}$ ] $^+$  204.1383, found 204.1388.

## ■ ASSOCIATED CONTENT

### Supporting Information

The Supporting Information is available free of charge on the ACS Publications website at DOI: 10.1021/acs.joc.5b01846.

Copies of  $^1\text{H}$ ,  $^{13}\text{C}$  NMR spectra and computational methods (PDF)

## ■ AUTHOR INFORMATION

### Corresponding Author

\*Phone: (650) 467-0236. E-mail: rene.olivier@gene.com.

### Present Address

$^{\S}$ I.A.S.: ETH Zurich Laboratory of Organic Chemistry, HCI F 306, Vladimir-Prelog-Weg 3, 8093 Zurich, Switzerland

### Notes

The authors declare no competing financial interest.



## ACKNOWLEDGMENTS

We thank Baiwei Lin and Christopher Tom for HMRS support and Yanzhou Liu for NMR support. We also thank Malcolm Huestis and Lauren Sirois for sharing relevant literature reviews in the preparation of this manuscript.

## REFERENCES

- (1) (a) Heathcock, C. H.; Blumenkopf, T. A.; Smith, K. M. *J. Org. Chem.* **1989**, *54*, 1548. (b) Lin, W.-H.; Xu, R.-S.; Wang, R.-J.; Mak, T. C. W. *J. Crystallogr. Spectrosc. Res.* **1991**, *21*, 189. (c) Fürstner, A.; Thiel, O. R. *J. Org. Chem.* **2000**, *65*, 1738.
- (2) (a) Heck, H. d'A.; Buttrill, S. E., Jr; Flynn, N. W.; Dyer, R. L.; Anbar, M.; Cairns, T.; Dighe, S.; Cabana, B. E. *J. Pharmacokinet. Biopharm.* **1979**, *7*, 233. (b) Hou, F. F.; Zhang, X.; Zhang, G. H.; Xie, D.; Chen, P. Y.; Zhang, W. R.; Jiang, J. P.; Liang, M.; Wang, G. B.; Liu, Z. R.; Geng, R. W. *N. Engl. J. Med.* **2006**, *354*, 131. (c) Narasimhan, M.; Bruce, T. O.; Masand, P. *Neuropsychiatr. Dis. Treat.* **2007**, *3*, 579.
- (3) Carraher, C. E., Jr *J. Chem. Educ.* **1978**, *55*, 51.
- (4) Casadei, M. A.; Galli, C.; Mandolini, L. *J. Am. Chem. Soc.* **1984**, *106*, 1051.
- (5) For a review on ring expansion for the formation of seven-membered rings, see: Kantorowski, E. J.; Kurth, M. *J. Tetrahedron* **2000**, *56*, 4317.
- (6) For a review on transition metal chemistry of cyclopropenes and cyclopropanes, see: Rubin, M.; Rubina, M.; Gevorgyan, V. *Chem. Rev.* **2007**, *107*, 3117.
- (7) For selected reviews on the cleavage of carbon–carbon bonds by transition metals, see: (a) Murakami, M.; Ito, Y. *Top. Organomet. Chem.* **1999**, *3*, 97. (b) Murakami, M.; Matsuda, T. *Chem. Commun.* **2011**, *47*, 1100. (c) Seiser, T.; Cramer, N. *Org. Biomol. Chem.* **2009**, *7*, 2835. (d) Marek, I.; Masarwa, A.; Delaye, P.-O.; Leibel, M. *Angew. Chem., Int. Ed.* **2014**, *53*, 2. (e) Laetitia, S.; Cramer, N. *Chem. Rev.* **2015**, *115*, 9410.
- (8) For a review on  $\beta$ -carbon elimination reactions, see: Aïssa, C. *Synthesis* **2011**, *2011*, 3389.
- (9) The Pd(0)-catalyzed carbon–carbon bond cleavage of electronically-activated 1,1-difluoro-2-arylcyclopropanes has been reported to lead to palladacyclobutane intermediates in the synthesis of 2-fluorinated allylic products; see: Xu, J.; Ahmed, E.-A.; Xiao, B.; Lu, Q.-Q.; Wang, Y.-L.; Yu, C.-G.; Fu, Y. *Angew. Chem., Int. Ed.* **2015**, *54*, 8231.
- (10) Palladium(0) has also been reported to effect carbon–carbon bond cleavage in highly activated cyclopropanes, such as 1,1,2,2-tetracyanocyclopropane, see: Lenarda, M.; Graziani, M.; Belluco, U. *J. Organomet. Chem.* **1972**, *46*, C29.
- (11) The platinum(0)-catalyzed rearrangement of highly strained oxaspirohexanes led to 3-methylenetetrahydrofurans via a similar proposed mechanistic pathway. Treatment of our reported substrates to platinum catalysis led to no desired product formation; see: Malapit, C. A.; Chitale, S. M.; Thakur, M. S.; Taboada, R.; Howell, A. R. *J. Org. Chem.* **2015**, *80*, 5196.
- (12) Surry, D. S.; Buchwald, S. L. *Chem. Sci.* **2011**, *2*, 27.
- (13) For discussions on anionic palladium(0) complexes, see: (a) Amatore, C.; Carré, E.; Jutand, A.; M'Barki, M. A.; Meyer, G. *Organometallics* **1995**, *14*, S605. (b) Amatore, C.; Jutand, A. *Acc. Chem. Res.* **2000**, *33*, 314.
- (14) Other carbonate, acetate, and phosphate bases also promoted the reaction and gave rise to conversions ranging between 38 and 97%. The use of NaOt-Bu with *t*-AmOH resulted in no product formation.
- (15) For a review on catalyst deactivation, see: Crabtree, R. H. *Chem. Rev.* **2015**, *115*, 127.
- (16) Siegbahn, P. E.; Blomberg, M. R. A. *J. Am. Chem. Soc.* **1992**, *114*, 10548.
- (17) For a review on trimethylenemethane cycloaddition chemistry, see: Yamago, S.; Nakamura, E. *Org. React.* **2002**, *61*, 1.
- (18) Trost, B. M. *Angew. Chem., Int. Ed. Engl.* **1986**, *25*, 1.
- (19) Binger, P.; Schuchardt, U. *Chem. Ber.* **1980**, *113*, 3334.
- (20) Suzuki, T.; Fujimoto, H. *Inorg. Chem.* **2000**, *39*, 1113.
- (21) (a) Nakamura, I.; Saito, S.; Yamamoto, Y. *J. Am. Chem. Soc.* **2000**, *122*, 2661. (b) Nakamura, I.; Siriwardana, A. I.; Saito, S.; Yamamoto, Y. *J. Org. Chem.* **2002**, *67*, 3445.
- (22) (a) Nakamura, I.; Itagaki, H.; Yamamoto, Y. *J. Org. Chem.* **1998**, *63*, 6458. (b) Siriwardana, A. I.; Kamada, M.; Nakamura, I.; Yamamoto, Y. *J. Org. Chem.* **2005**, *70*, 5932.
- (23) Hay, P. J.; Wadt, W. R. *J. Chem. Phys.* **1985**, *82*, 299.
- (24) Further details are available in the [Supporting Information](#).
- (25) For selected examples, see: (a) Hicks, J. D.; Hyde, A. M.; Cuezva, A. M.; Buchwald, S. L. *J. Am. Chem. Soc.* **2009**, *131*, 16720. (b) Düfert, M. A.; Billingsley, K. L.; Buchwald, S. L. *J. Am. Chem. Soc.* **2013**, *135*, 12877. (c) Zhou, Y.; Zhang, X.; Liang, H.; Cao, Z.; Zhao, X.; He, Y.; Wang, S.; Pang, J.; Zhou, Z.; Ke, Z.; Qiu, L. *ACS Catal.* **2014**, *4*, 1390.
- (26) Charles, M. D.; Schultz, P.; Buchwald, S. L. *Org. Lett.* **2005**, *7*, 3965.
- (27) Li, Z.; Fu, Y.; Guo, Q.; Liu, L. *Organometallics* **2008**, *27*, 4043.
- (28) Previous computational and NMR studies identified mono-ligated LPd(0) as the active catalyst for oxidative addition reactions with biarylphosphine ligands SPhos and X-Phos. A similar  $\eta^1$  arene-Pd interaction was calculated for these structures, see: Barder, T. E.; Biscoe, M. R.; Buchwald, S. L. *Organometallics* **2007**, *26*, 2183.
- (29) All reported energies are relative to the sum of the energy of the separated educt **20** and the catalyst **27**.
- (30) Peng, C.; Ayala, P. Y.; Schlegel, H. B.; Frisch, M. J. *J. Comput. Chem.* **1996**, *17*, 49.
- (31) Frisch, M. J.; et al. *Gaussian 03*, revision D.01; Gaussian, Inc.: Wallingford, CT, 2009.
- (32) The calculated energy barriers that we have obtained for the C–N bond and the C–C bond oxidative addition to the Pd(0) catalyst are in agreement with the values obtained in a previous report describing a related Pd(0)-catalyzed process that involved an initial formation of a palladacyclobutane intermediate that subsequently rearranged to a  $\pi$ -allyl complex, see ref **9**.
- (33) The rearrangement was attempted at room temperature to form caprolactam **6**, and no observable amount of product was observed under catalytic conditions. However, under stoichiometric conditions with 1 equiv of the palladium complex at room temperature, **6** was formed in 7% conversion as determined by  $^1\text{H}$  NMR analysis of the crude reaction mixture. A catalyst turnover number of 0.07 at room temperature is in line with our calculated rate-determining energy barrier.
- (34) Anslyn, E. V.; Dougherty, D. A. Postulates and principles related to kinetic analysis. *Modern Physical Organic Chemistry*, 1st ed; University Science Books: Sausalito, CA, 2006; pp 374–379.
- (35) All azaspirocyclic lactam starting materials can be obtained in one step from the corresponding  $\gamma$ -cyanoester using a chemoselective titanium-mediated cyclopropanation reaction, see: Bertus, P.; Szymoniak, J. *Synlett* **2003**, 265.